Response to the Comments of the Reviewer

(1) The authors have done a strong job of revising their manuscript; I commend them on their work and apologize for my extreme tardiness in getting this assessment completed. I suggest that this should be publishable once the authors address remaining comments not addressed, or raised through the revisions.

We have done our best to address the comments and suggestions of the reviewer. Our responses and changes to the manuscript (in black) follow each comment of the reviewer (in blue).

(2) As a general thought, I would encourage the authors to consider the sensitivity of their results to the one very clear "outlier" high absorption point in their unexplained absorption vs. ELVOC concentration plots. This point is undoubtedly having an outsized effect on the fits, especially the R^2 value. This is not critical, but perhaps of interest. Additional comments follow.

This period characterized by high unexplained absorption and high ELVOC concentration is indeed important for the results. We do not think that though that this period should be described as an outlier. We have repeated the analysis excluding this period and the R^2 between unexplained absorption and ELVOC levels is lower, but still relatively high at 0.41. We have added this comment in the revised manuscript.

(3) The authors added mention of factors that can affect the MAC of pure BC to the intro; I suggest the authors support these contentions with references that specifically demonstrate from observations (not calculations) that the MAC is size dependent. This is certainly true if spherical particle Mie theory is used, but it is less clear this is the case for fractal particles; for example, RDG theory yields a size-independent MAC. Also, just a note that neither RDG nor Mie rely on knowledge of particle morphology; the former requires only the size of the primary spherule, but not the morphology (page 2)

We have followed the reviewer's suggestion and added references to the experimental work of Radney et al. (2014), Dastanpour et al. (2017), and Forestieri et al. (2018) together with a brief discussion. We have also rephrased the text to clarify what is needed by the RDG and the Mie theory.

(4) L223: The authors report a positive correlation for an R=0.31, corresponding to an $R^2 = 0.096$. This is hardly a positive correlation. I suggest that the authors perform a significance test to determine whether their correlation coefficient is significantly different from zero at some level. I am not convinced that the authors can really conclude that "the measurements suggested a positive correlation", or that the R value reported is not strongly influenced by the two outliers at low NRPM/rBC values. The same goes for the small R^2 values reported on L275/276.

We have performed a significance test and confirmed that these results are statistically significant at the 5% level. This information has been added to the paper.

(5) It would be very useful for future reference if the authors were to report the SSA value they measured for the fullerene soot. Also, the authors cite Lack et al. (2012) for the PAX uncertainty (page 5). However, Lack et al. did not use a PAX, they used a CRD-PAS and calibrated in a totally different manner than by which the PAX is calibrated. It is not clear that the uncertainties are translatable; I think the authors need to argue that the uncertainties translate between these different instruments that were calibrated in different ways and have very different sensitivities.

This is a valid point. We have rewritten this discussion of the uncertainty of the PAX measurements based, this time, on the work of Nakayama et al. (2015) who characterized the uncertainty of a Photoacoustic Extinctiometer (PAX) and a three wavelength Photoacoustic Soot Spectrometer. The measurement uncertainties for the PAX were less than 10%. The SSA value measured for the fullerene has been added to the text.

(6) L239: I suggest the authors provide more details regarding how they determined the values reported in Fig. S11 from the LEO method. LEO gives a result for every particle. They report an average value. But is the distribution normally distributed? And, for what size particle were these coatings determined? There are some important aspects to the LEO method with respect to how it is applied across the size distribution owing to differences in the smallest size particle measured by incandescence versus scattering in the SP2. Are these coating thicknesses from a particular size range?

We estimated the coating thickness for every BC particle with the LEO method. The average coating thickness for each period shown in Fig. S11 corresponds to the mean BC particle size ($\pm$ 5 nm) for the same period. This information has been added to the revised paper.

(7) Additionally, I have some concerns with the real discussion of the LEO method being left to the "uncertainty" analysis. We know for a fact that the NRPM/BC overestimates the coating thickness. Considering the LEO method is not just looking at "uncertainty;" it is arguably a fundamentally better estimate (despite the limitations of the method). This does not seem so much like an "uncertainty analysis" to me, as it is an alternative consideration. I strongly suggest integrating the LEO results with the NRPM/BC results throughout. It should be reasonably straightforward to show both the NRPM/BC and LEO-derived results together in the main text figures and to discuss them together. As a general point, I suggest that a better title than "Uncertainty analysis" would be "sensitivity analysis." The vast majority of the aspects considered in this section are assessing sensitivities of the results to methodological assumptions, which is not the same as an uncertainty assessment. It is more of a robustness assessment. Regardless, this is a welcome addition to the paper.

We agree with the point of the reviewer. We have moved the analysis using the LEO approach for the calculation of the coating thickness to Sections 4.2 and 4.3. We have also renamed the new section to "Sensitivity analysis".

(8) I appreciate the authors' addition of the R^2 values as a function of wavelength for absorption vs. BC. I suggest changing "rather inconclusive" simply to "inconclusive." I'll note also that they report only in the supplemental but not the main text the value at the longest wavelength, for which the R^2 is quite a bit lower than at higher wavelengths.

We have changed the characterization to "inconclusive" as suggested by the reviewer. The R^2 between the high wavelength b_{abs} (λ=950 nm) and the rBC mass has been added to the main text.

(9) P14: I suggest that the authors in their first sentence change it to "between the measured and the reference value" rather than "theoretical value," in line with my previous concern that it appeared the authors were comparing their observations with a calculated ("theoretical") value. The Bond et al. value is not theoretical—it is explicitly derived from experiments.

We have rephrased this sentence to avoid confusion and we now discuss the "reference value".

(10) P15: The average predicted MAC405 is likely not lower than the measured value once uncertainties are accounted for. This should be noted. The authors should provide statistical evidence that the predicted value is lower, based on e.g. a t-test or some other appropriate test. We have followed the suggestion of the reviewer and analyzed the statistical significance of the difference between the average measured and estimated value. The MAC uncertainty due to the corrections introduced by the size limitation of the SP2 was minor and that by the PAX measurements was less than 10%. Based on these an uncertainty of the measured MAC$_{405}$ approximately equal to 10% has been estimated. The t-test suggested a p=0.078 for the predicted value being less than the measured one. These points have been added in the revised manuscript.

(11) P14: I also suggest that the authors modify their discussion in relation to the Gyawali et al. (2009) study to indicate that those were theoretical values obtained via spherical particle Mie theory, which might not yield (and probably does not yield) the correct size dependence—which is what gives rise to the large variation in the AAE with size in that paper and others that have followed. For the Lui et al. study cited, the authors here should not just note that the AAE decreases with size (for more complex calculations) but that it decreases to only ~0.8 at the lower end for their realistic calculations. The authors should be more specific than saying "relatively low values of AAE should be expected." How low is low? If 0.8 for collapsed BC is expected, then an observed value of 1 still indicates a relatively small contribution of brown carbon.
We have added in the revised paper the information suggested by the reviewer regarding the Gyawali et al. (2009) and Lui et al. (2018) studies. According to the results of Gyawali et al. (2009), the average AAE for the present study based on the core diameter measured and the estimated coating thickness can range from 1 to 1.25. This has also been added in the revised version.

(12) P15: I find the statement that "The association of BrC with material of lower volatility away from its sources has been reported in a number of studies focusing on biomass burning (Saleh et al., 2014; Wong et al., 2019)," unclear. The Saleh study is a laboratory study on biomass burning particles; it is by definition right by the source. But, they did consider the influence of simulated photochemical aging. The Wong et al. study is also a laboratory study, but one that did consider photo-aging of BrC. If the authors here mean that the Saleh and Wong et al. photochemically aged their laboratory samples and this means "away from its sources" I suggest they be more specific. This is a valid point. We have rephrased this sentence replacing the statement "away from its sources" with "photochemical aged aerosol" to be more precise.

(13) P17: There is a typo: the RI should be + 0.79i, not 0.679i.
The typo has been corrected.

(14) Data Availability: In line with current best practice and expectations for articles published in ACP, I suggest that the authors archive their data from the publicly funded study in an accessible archive prior to the publication of this work.
A significant fraction of the result of this field study has not been published yet. A couple of papers are under preparation. All the results will be archived in an accessible repository after the completion of the publication process. In the meantime, the results presented in the paper are archived in a restricted repository and are available upon request.

(15) Presentation of Literature Results: Upon reading again, I have a few concerns over how the previous literature is presented. Specific comments follow here:
L38: The authors should clarify that the measured Eabs accounts for the combined effects of lensing and BrC. This would help set up the discussion that follows better, especially when they report measurements of Eabs from different studies without clearly delineating the relative contributions of lensing and BrC.
We now clarify in the revised paper that the measured Eabs accounts for the combined effects of both lensing and BrC.

(16) L49: I suggest it would be fairer to say that studies have found a wide range of effects.
The text has been rephrased following the reviewer's suggestion.

(17) L50: The authors misstate the results of Liu. Here, the authors report the results from the TD, but Liu et al emphasize that the MAC-based method is superior. Their 405 nm value is larger than the 781 nm value, when viewed this way. And this is largely a result of BrC absorption, with lensing making some contribution. I suggest this be revised to reflect the results of Liu et al. more accurately.
Additional information about the findings and conclusions of Liu et al. (2005) has been added to the text.

(18) General comment on presentation of literature results: In general, I suggest the authors report the uncertainties associated with each of the specific Eabs values they mention. There can be a wide variability/range of values for a given mean value. Or, they should clarify that these are means. I also suggest that they introduce greater consistency in terms of attributing different effects to lensing versus brown carbon. For example, for the Zhang et al. 2018a study, they mention two wavelengths with no mention of attribution. But for the Lack et al. (2012) study, they mention contributions of BrC.
We do clarify now that the reported Eabs values are averages of a range of values. The variability is also reported when available. We have tried to improve the consistency of the reported effects in the literature review. Unfortunately, we are limited by the analysis performed in each study. For example, in a number of studies there is no effort to quantify the contribution of BrC.

(19) For the Liu et al. (2017) study, the authors might clarify that above Rbc = 3 the enhancement is not only "significant," but that they observed a continual variation in Eabs with increasing Rbc.
We have added the suggested clarification to the revised paper.

(20) For the Cappa et al. (2012) study, I believe they also report values using the MAC method, and find results similar to the TD method.
The above information has been added.

(21) L74: Hearly should be Healy.
The typo has been corrected.

(22) Rbc: The authors should clarify that different methods are used to determine Rbc. For Liu et

al. (2017), for example, it is based on single particle SP2 measurements. But for most other studies mentioned, the Rbc (if measured at all) is an ensemble average.
We have added the requested information about the method used to measure the R_{BC}.

(23) For McMeeking et al. (2014), the absorption enhancement was negligible up to Rbc = 10. Not just below Rbc = 1.
The suggested clarification has been added.

(24) L59: cite should be site.
The text has been corrected.

(25) L137: The distributions were almost certainly not fit with a Gaussian. They were fit with a log-normal distribution. (If they were actually fit with a Gaussian, this needs to be justified.)
The data were fitted using a log normal distribution. The text has been corrected.

References

Dastanpour, R., Momenimovahed, A., Thomson, K., Olfert, J., and Rogak, S.: Variation of the optical properties of soot as a function of particle mass, Carbon, 124, 201–211, 2017.

Forestieri, S. D., Helgestad, T. M., Lambe, A. T., Renbaum-Wolff, L., Lack, D. A., Massoli, P., Cross, E. S., Dubey, M. K., Mazzoleni, C., Olfert, J. S., Sedlacek Iii, A. J., Freedman, A., Davidovits, P., Onasch, T. B., and Cappa., C. D.: Measurement and modeling of the multiwavelength optical properties of uncoated flame-generated soot, Atmos. Chem. Phys., 18, 12141–12159, 2018.

Nakayama, T., Suzuki, H., Kagamitani, S., Ikeda, Y., Uchiyama, A., and Matsumi, Y.: Characterization of a Three Wavelength Photoacoustic Soot Spectrometer (PASS-3) and a Photoacoustic Extinctiometer (PAX). J. Meteorol. Soc. Jpn., 93,285–308, 2015.

Radney, J. G., You, R., Ma, X., Conny, J. M., Zachariah, M. R., Hodges, J. T., and Zangmeister, C. D.: Dependence of Soot Optical Properties on Particle Morphology: Measurements and Model Comparisons, Environ. Sci. Technol., 48, 3169–3176, 2014.

1 **Aerosol light absorption and the role of extremely low volatility organic**

2 **compounds**

3

4 Antonios Tasoglou[1,5], Evangelos Louvaris[2,3], Kalliopi Florou[2,3] Aikaterini Liangou[2,3], Eleni

5 Karnezi[1] Christos Kaltsonoudis[4], Ningxin Wang[1], Spyros N. Pandis[1,2,3]

6 [1]Department of Chemical Engineering, Carnegie Mellon University, Pittsburgh
7 [2]Department of Chemical Engineering, University of Patras, Patras, Greece
8 [3] Institute of Chemical Engineering Sciences (ICE-HT), FORTH, Patras, Greece
9 [4]Department of Mechanical Engineering, Carnegie Mellon University, Pittsburgh, United States
10 [5]RJ Lee Group, Inc., Monroeville, United States

11

12 **Abstract**

13 A month-long set of summertime measurements in a remote area in the Mediterranean is

14 used to quantify aerosol absorption and the role of black and brown carbon. The suite of

15 instruments included a high-resolution Aerosol Mass Spectrometer (HR-ToF-AMS), and a

16 Scanning Mobility Particle Sizer (SMPS) both coupled to a thermodenuder and an aethalometer,

17 a photoacoustic extinctiometer (PAX$_{405}$), a Multi-Angle Absorption Photometer (MAAP), and a

18 Single Particle Soot Photometer (SP2).

19 The average refractory black carbon (rBC) concentration during the campaign was 0.14 μg

20 m^{-3}, representing 3% of the fine aerosol mass. The measured light absorption was two or more

21 times higher than that of fresh black carbon (BC). Mie theory indicated that the absorption

22 enhancement due to the coating of BC cores by non-refractory material could explain only part of

23 this absorption enhancement. The role of brown carbon (BrC) and other non-BC light-absorbing

24 material was then investigated. A good correlation (R^2=0.76) between the unexplained absorption

25 and the concentration of extremely low volatility organic compounds (ELVOCs) mass was found.

26

27 **1. Introduction**

28 Atmospheric aerosol may influence climate in two ways: directly through scattering and

29 absorbing radiation, and indirectly through acting as cloud condensation nuclei (IPCC, 2011)

30 Black carbon is the dominant light absorbing aerosol component. BC is a distinct type of

31 carbonaceous material that is formed mainly during combustion processes. In addition, some

32 organic aerosol (OA) has the ability to absorb sunlight. The OA with strong light absorption is

33 called brown carbon (BrC) (Andreae et al., 2006).

34 The absorption of BC depends on its mixing state (Liu et al., 2015, 2017). Usually, BC is

35 coated with scattering material causing its light absorption to increase due to the lensing effect

36 (Fuller et al., 1999; Jacobson, 2001; Bond et al., 2006; Lack and Cappa, 2010). The absorption

37 enhancement (E_{abs}) is defined as the ratio of the aerosol absorption coefficient (b_{abs}) over the b_{abs}

38 of the pure BC particles. The E_{abs} accounts for the combined effects of lensing and the presence of

39 BrC. This enhancement can also be calculated by the ratio of the equivalent mass absorption cross-

40 sections (MAC). The MAC is defined as the ratio of b_{abs} over the BC mass. The MAC of pure,

41 uncoated BC at a specific wavelength depends both on the size distribution of the particles, but

42 also on their morphology (fresh aggregates versus collapsed more spherical structures). Forestieri

43 et al. (2018) measured the~~a~~ size dependent MAC for particles with a diameter lower than 160 nm.

44 Radney et al. (2014) and Dastanpour et al. (2017) showed that the MAC is proportional to particle

45 mass. Based on Bond et al. (2006) pure BC particles in the 10-350 nm diameter range have an

46 expected MAC$_{550}$ =3.9-6.8 m^2 g^{-1} and~~or~~ MAC$_{405}$ =5.3-9.2 m^2 g^{-1}. The E_{abs} can be measured by

47 using a thermodenuder (TD) for the removal of the non-refractory coating material from the BC-

48 containing particle~~s,~~ or it can be estimated using ~~a~~ theoretical model~~s~~ (for example Mie or

49 Rayleigh-Debye-Gans theory) if the size of the primary spherules ~~particle morphology~~ is known.

50 Incomplete removal of the non-refractory material in the TD can lead to underestimation of the

51 E_{abs} (Healy et al., 2015; McMeeking et al., 2014).

52 Previous studies have demonstrated that lensing has a wide range of ~~strong~~ effects on the

53 light absorption of BC. Liu et al. (2015) quantified~~reported~~ the E_{abs} in a rural area near London

54 during the winter. ~~They used two methods to find the E$_{abs}$.~~ Using the TD method they found a

55 campaign--average E_{abs} of 1.3 at ~~wavelength (λ) equal to~~ 405 nm and 1.4 at 781 n~~m. They also

56 estimated the In~~ E_{ab} ~~the second method they~~ combining~~pared~~ their measurements with a reference

57 MAC from the literature ~~to estimate the E$_{abs}$:~~m in a rural area near London during the winter~~. At

58 the large wavelength the two methods agreed, but this was not the case at the lower ~~but at the

59 small~~ wavelength ~~the difference was significantly higher. They argued that the E$_{abs}$ calculated

60 using the reference MAC was more accurate.~~ In addition, they showed that there was ~~is a

61 continu~~ous al~~change~~variation~~ in E_{abs} with increasing R_{BC}. The R_{BC} was defined as the ratio of the

62 non-rBC mass to the rBC mass in BC-containing particles, measured by the SP-AMS. Finally, this

63 study ~~They also~~ suggested that the lower volatility BrC ha~~d~~s stronger absorption than the semi-

64 volatile BrC. Knox et al. (2009) performed measurements in downtown Toronto, during the

65 wintertime using a TD at 340 $^{\circ}$C. They reported an average E_{abs} of 1.43 for fresh particles, based

66 on thermal OC/EC and photoacoustic measurements. Liu et al. (2017) combined laboratory

67 experiments with diesel exhaust emissions and ambient measurements to show that particles with

68 a ratio of ~~non-refractory PM to BC mass (R_{BC})~~ less than 1.5 (typical for traffic emissions) had a

69 negligible lensing effect. The R_{BC} was measured by combining an AMS and an SP2. When the

70 R_{BC} was above 3, lensing caused significant enhancement of the absorption of BC. They observed

71 a ~~continual variation~~continuous change in E_{abs} with increasing R_{BC}. Zhang et al. (2018a) presented

72 three years of measurements in a suburban s~~e~~ite outside Paris, France, influenced by both fresh

73 and aged air masses. On average they found an E_{abs}=2.07 at 370 nm, and an E_{abs}=1.53 at 880 nm.

74 They calculated the E_{abs} by measuring the absorption coefficient (b_{abs}) with an aethalometer, while

75 the elemental carbon (EC) was measured with thermal methods using daily filters. Zhang et al.

76 (2018b) presented measurements in Beijing, China during wintertime. Using aethalometer

77 measurements, refractory and non-refractory particle size distributions and Mie theory, they

78 calculated that the lensing effect led to an E_{abs} ranging from 1.5 to 2 on average at 880 nm. Zanatta

79 et al. (2018) found an average E_{abs} equal to ~~=~~1.54 at 550 nm for measurements at the Zeppelin

80 Arctic Station. Lack et al. (2012) analyzed measurements of biomass burning plumes near Boulder,

81 CO during summertime. Using a TD at 200 $^{\circ}$C, they found E_{abs} values as large as 2.5 at 404 nm

82 and 1.7 at 532 nm. Using the absorption Angström exponent (AAE) and Mie theory calculations

83 they showed the presence of BrC.

84   Some studies have argued that Mie theory may overestimate the E_{abs}. Cappa et al. (2012)

85 suggested that the absorption enhancement of BC in California in the summertime was low with

86 average values equal to 1.13 at 405 nm and 1.06 at 532 nm for R_{BC}>10. ~~R_{BC} measured by the SP-~~

87 ~~AMS and the SP2.~~ For their measurements they used a TD operated at 225-~~$^{\circ}$C and~~250 $^{\circ}$C.

88 ~~Additional E_{abs} values were presented calculated by the ratio of the MAC measured over a~~

89 ~~reference MAC at each wavelength. The TD related E_{abs} was within the rage of the reference MAC~~

90 ~~based E_{abs}.~~ Hea~~r~~ly et al. (2015) also reported practically no enhancement in the BC absorption at

91 781 nm and an average E_{abs}=1.19 at 405 nm in Toronto, Canada during summertime. During a

92 period associated with wildfires the same authors measured R_{BC}=6.9 and an average E_{abs}=1.39 at

93 405 nm. ~~R_{BC} measured by the SP-AMS.~~ They argued that there was little evidence of the lensing

94 effect, and that BrC was driving the E_{abs}. Cappa et al. (2019) performed measurements in Fresno,

95 CA during wintertime and Fontana, CA during summertime. They found that in Fresno there was

96 absorbing OA, BrC, which was related to biomass burning OA and nitrate-associated OA. In

97 Fresno, they reported average E_{abs} of 1.37, 1.22 and 1.1 at wavelengths equal to 405, 532, 781 nm,

98 respectively, for R_{BC} ranging from 1 to 4. ~~R_{BC} measured by the SP-AMS and the SP2.~~ In Fontana

99 the E_{abs} was lower with values of 1.1 at 405 nm and 1.07 at 532 nm. Laboratory measurements of

100 McMeeking et al. (2014) for biomass burning aerosol indicated higher absorption in lower

101 wavelengths compared to higher ones and thus the presence of BrC. The~~No~~ enhancement of the

102 absorption was ~~observed~~ negligible at R_{BC}<1~~0~~. On average they found an E_{abs} equal to 1.25 at 781

103 nm with a maximum value of E_{abs}=4 for R_{BC}>10. ~~R_{BC} measured by the SP-AMS and the SP2.~~

104 Recent studies have suggested that the absorption efficiency of OA could be related to its

105 volatility. Saleh et al. (2014) in their laboratory biomass burning experiments showed that almost

106 all absorbing OA was associated with extremely low volatility compounds (ELVOCs), with an

107 effective saturation concentration C^* of 10^{-4} µg m^{-3}. In addition, Saleh et al. (2018) using controlled

108 combustion experiments showed that the absorption activity of BrC is proportional to its molecular

109 size.

110 Despite the significant progress in understanding the absorption of atmospheric fine aerosol

111 there are still remaining questions regarding both the absorption enhancement of black carbon and

112 the absorption of OA as the aerosol evolves in the atmosphere. In this study we try to address these

113 issues for aerosol that has been aged in the atmosphere for at least a few days before arriving at

114 the island of Crete in the Eastern Mediterranean.

115

116 **2. Experimental Methods**

117 A remote location in the Eastern Mediterranean was used for the study of the absorption

118 and volatility of aged carbonaceous aerosol. The area is characterized by intense photochemistry,

119 especially during the summer (Pikridas et al., 2010) and is affected by pollutants transferred from

120 continental Europe, Turkey, Greece and Africa (Mihalopoulos et al., 1997; Lelieveld et al., 2002;

121 Kalivitis et al., 2011; Bougiatioti et al., 2014). Previous measurements have shown that the OA

122 reaching the area is highly oxidized regardless of its origin (Hidlebrandt et al., 2010; 2011). Lee

123 et al. (2010) showed that these oxidized organic compounds have much lower volatility than fresh

124   SOA. Long-term measurements in the region have revealed relatively high light absorption and
125   scattering by aerosol during the summer (Kalivitis et al., 2011; Vrekoussis et al., 2005).

126   The FAME-16 field campaign took place from May 9 to June 2, 2016. Measurements were
127   conducted at the Finokalia Station (35° $20'$ N, 25° $40'$ E, 250 m asl), a remote site on the island of
128   Crete in Greece (Mihalopoulos et al., 1997). The nearest large city is Heraklion with 150,000
129   inhabitants located 50 km west of Finokalia (Kouvarakis et al., 2000). There are no local sources
130   near the station, allowing the investigation of aged OA from different source regions. During this
131   study, two Saharan dust events occurred from May 12 till May 15 and May 21 till May 22.

132   A Scanning Mobility Particle Sizer (SMPS, TSI classifier model 3080, CPC model 3775)
133   was used to measure the number and the size distribution of the particles. The aerosol flow was
134   set at 1 L min^{-1} and the sheath flow at 5 L min^{-1}. The sampling time was 3 min.

135   The mass concentration and the chemical composition of the particles were monitored
136   using a High-Resolution Time-of-Flight Aerosol Mass Spectrometer (HR-ToF-AMS, Aerodyne
137   Research, Inc.). SQUIRREL 1.56D and PIKA v1.15D were used for the data analysis, while for
138   the elemental ratio calculations the improved ambient calculation approach of Canagaratna et al.
139   (2015) was used. The HR-ToF-AMS was operated in V-mode with a sample time of 3 min. The
140   collection efficiency of the HR-ToF-AMS was calculated using the algorithm of Kostenidou et al.
141   (2007). The average CE was 0.64±0.2. Positive matrix factorization (PMF) analysis (Lanz et al.,
142   2007; Paatero and Tapper, 1994; Ulbrich et al., 2009) was performed using as input the high
143   resolution OA mass spectra and the mass-to-charge ratios (m/z) from 12 to 200.

144   A Single Particle Soot Photometer (SP2, Droplet Measurement Technologies) was used to
145   measure the BC size distribution and concentration. The SP2 had 8-channels and included a 1064
146   nm Nd:YAG laser operating at 4 V and 3400 A. The instrument was calibrated using fullerene
147   soot (Alfa Aesar, stock 40971, lot L20W054, SSA=0.4) (Gysel et al., 2011). The calibration of the
148   SP2 was verified in separate experiments using a centrifugal particle mass analyzer (CPMA,
149   Cambustion). The SP2 mode mass and the CPMA mode mass were in good agreement with an
150   R^2=0.99 (Saliba et al., 2016). The data were analyzed using the Probe Analysis Package for Igor.
151   In our measurements, the number concentration of BC was low (<10,000 particles cm^{-3}), and thus
152   it was assumed that there were no coincidence artifacts in our measurements. The scattering
153   measurement was calibrated using monodisperse polystyrene latex (PSL) spheres. The BC number
154   concentration distributions measured by the SP2 were fitted using a log-normal Gaussian

distribution to account for particles smaller than the SP2 detection limit of approximately 50 nm (Ditas et al., 2018). This extrapolation resulted in an increase of the BC mass concentration by 3-8% (Figure S9), therefore the uncertainty introduced by BC outside the measurement window was minor.

A photoacoustic extinctiometer (PAX, Droplet Measurement Techniques) with a blue (405 nm) laser was used to measure the absorption (b_{abs}) and the scattering (b_{scat}) coefficients. Fullerene soot and PSL spheres were used to calibrate the absorption and scattering signals, respectively. An activated carbon denuder was placed in front of the PAX to remove NO_2. The b_{abs} measurement by the PAX has an uncertainty of less than 10% ~~for the b~abs~ measurement~~ (Nakayama ~~Lack~~ et al., 201~~2~~5). Furthermore, a seven wavelength aethalometer (AE31, Magee Scientific) was used to measure the b_{abs} at 370, 470, 520, 590, 660, 880 and 950 nm and to calculate the absorption Angstrom exponent (AAE), which describes the wavelength dependence of the b_{abs}. The aethalometer measurements were corrected for scattering and multiple scattering artifacts following Saleh et al. (2014) and Tasoglou et al. (2017) using the corrections suggested by Weingartner et al. (2003) and Kirchstetter and Novakov (2007). High relative humidity (>70%) can introduce measurement artifacts in the measurement absorption coefficient by filter- based techniques or photoacoustic methods (Arnott et al. 2003). A diffusion drier was used upstream of the optical measurements. The campaign average temperature and relative humidity were 22±4 $^{\circ}$C and 53±19 %, respectively. The measurement station had a temperature-control system maintaining the temperature at approximately 25 $^{\circ}$C.

The thermodenuder (TD) used in this study, was placed upstream of the HR-ToF-AMS and the SMPS. The TD design was similar to that developed by An et al. (2007) and is described by Louvaris et al. (2017). The TD was operated at temperatures ranging from 25 $^{\circ}$C to 400 $^{\circ}$C using several temperature steps from 25 $^{\circ}$C to 200 $^{\circ}$C over several hours and then rapidly (in 20 min) increasing its temperature to the 375-400 $^{\circ}$C to investigate the presence of ELVOCs. One complete cycle from 25 to 400 $^{\circ}$C and back to 25 $^{\circ}$C lasted approximately 10 h. Sampling was alternated between the ambient line and the TD line every 3 minutes using computer-controlled valves. Changes in particle mass concentration, composition, and size due to evaporation in the TD were measured by the HR-ToF-AMS and the SMPS resulting in thermograms of OA mass fraction remaining (MFR) as a function of TD temperature. The OA MFR was calculated as the ratio of organic mass concentration of a sample passing through the TD at time t_i over the average mass

186   concentration of the ambient samples that passed through the bypass line at times t_{i-1} and t_{i+1}. The

187   sample residence time in the centerline of the TD was 14 s at 25 °C, corresponding to an average

188   residence time in the TD of 28 s. The MFR values were corrected for particle losses in the TD due

189   to diffusion and thermophoresis. To account for these losses, sample flow rate as well as size- and

190   temperature-dependent loss corrections were applied following Louvaris et al. (2017)

191   corresponding to the operating conditions during the campaign. Less than 20% of the particulate

192   matter was lost in the TD at temperatures up to 100°C. The losses increased at higher temperatures.

193   and at 400 °C approximately 50% of particles larger than 50 nm was lost. The uncertainty

194   introduced by the loss correction was approximately 20% (Gkatzelis et al., 2016; Louvaris et al.,

195   2017). The final step of the data analysis was to average the corrected for CE and TD losses MFR

196   data based on temperature bins of 10°C. The MFR calculation assumes implicitly that the OA

197   concentration remains constant during the measurement period. To ensure that this condition is

198   satisfied, if two consecutive OA ambient mass concentrations differed by more than 25%, the

199   corresponding MFR was not included in the analysis. Also, in order to ensure that the temperature

200   was constant during the measurement, the absolute difference between the two samples had to be

201   less than 5°C. If this difference for a TD sample was higher, then the sample was not included in

202   our analysis. The same approach was used also for the factors resulting from the PMF analysis of

203   the AMS spectra. However, in this case a minimum concentration threshold of 0.1 $\mu g\ m^{-3}$ was used

204   for the ambient concentrations together with the criterion of the stability of the ambient

205   concentrations during the sampling period. MFR values corresponding to concentrations of the

206   PMF factors below this threshold were not included in the dataset. Approximately 75% of the OA

207   samples satisfied all these constraints and were used in the analysis. The corresponding

208   percentages were 65% and 70% for the two identified PMF factors. In the present work the

209   complete datasets will be analyzed together, averaging the corresponding measurements. More

210   details regarding the data analysis and the sensitivity tests of the TD measurements are provided

211   in the supplementary information.

212   The concentrations of gas-phase pollutants were measured using a Proton-Transfer

213   Reaction Mass Spectrometer (PTR-QMS 500, Ionicon Analytik) and gas monitors. The PTR-MS

214   was calibrated with a standard gas mixture of VOCs. The concentration of O_3 was measured using

215   a continuous O_3 analyzer (Thermo Scientific, 49i) and the concentrations of nitrogen oxides were

216   measured using a NO/NO$_2$/NO$_x$ analyzer (Thermo Scientific, 42i-TL).

217

3. Theoretical Analysis Methods

The dynamic TD evaporation model of Riipinen et al. (2010) together with the uncertainty estimation algorithm of Karnezi et al. (2014) were used for the determination of the OA volatility distribution. Inputs for the model included the ambient OA concentration, the OA density calculated by the algorithm proposed by Kostenidou et al. (2007), the initial average particle size, TD temperature, the MFR values, and TD residence time. In the volatility basis set framework of Donahue et al. (2006), the volatility distribution is represented with a range of logarithmically spaced C^* bins along a volatility axis. In this study 6 bins with variable mass fractions were chosen. For this 6-bin solution, the best 2% of the mass fraction combinations with the lowest error were used to estimate the average mass fraction along with their corresponding standard deviation for the uncertainty of each bin. Additionally the parameters that affect indirectly the calculated volatility such as the effective vaporization enthalpy (ΔH_{vap}), and the effective accommodation coefficient (a_m) were estimated following Karnezi et al. (2014). Additional information regarding the data analysis of the TD measurements are in the supplemental information (sections S1 and S2).

A Mie theory model based on the work of Bohren and Huffman (1983) was used to calculate the theoretical MAC and E_{abs} at 405 nm assuming a spherical core-shell morphology (China et al., 2015). The assumption that all BC particles were coated and had obtained a relatively spherical shape can be justified by the lack of any local sources and the fact that all particles reaching the site had been heavily processed in the photochemically active summertime atmosphere of the Eastern Mediterranean. PMF analysis of the OA AMS spectra did not show any fresh emissions like HOA or BBOA and no acetonitrile was detected. FLEXPART analysis confirmed that the air masses measured were transferred from long distance areas (30% continental Greece and the Balkans, 13% Aegean, 24% Africa, 33% Italy/Sicily). The measurements suggested a positive correlation (R=0.31) between the MAC_{405} and the ratio of non-refractory PM_1 to rBC with an intercept of 12.1 m^2 g^{-1} (Figure S10).

For the BC core we assumed a refractive index of the core $n_{rBC}=1.85+0.71i$ (Bond et al., 2006) and a density of 1.8 g cm^{-3} (Mullins and Williams, 1987; Park et al., 2004; Wu et al., 1997). A non-absorbing coating of the BC core was assumed, with a refractive index of $n_{OA} = 1.55$ (Bond and Bergstrom, 2006). The total aerosol effective density used was calculated based on the SMPS

13

248 and HR-ToF-AMS distributions. The average effective density for the campaign was 1.66±0.11 g

249 cm^{-3}. The size distribution of the BC cores was provided by the SP2 and the corresponding

250 measured rBC size distributions including the extrapolation to smaller sizes outside the SP2

251 measurement window.

252   The coating thickness in the base case calculation was estimated based on the assumption

253 that the BC material is internally mixed with the non-refractory aerosol species (Saliba et al.,

254 2016). The SMPS size distributions were used to estimate the ratio of the total aerosol mass over

255 the BC mass as measured. 1-hour averaged data were used as inputs in the model. In order to

256 provide a better constraint for the analysis, the average coating thickness for each period of the

257 corresponding mean~~r~~ BC cores (± 5 nm) was ~~also~~ estimated using the leading-edge-only (LEO) fit

258 method (Gao et al. 2007) and the SP2 data. The thicknesses as expected were lower than those

259 resulting from the internal mixing assumption, but were still significant (Figure S11). ~~Repeated~~

260 Mie theory calculations using the coating thickness based on the LEO fit method were also

261 performed.~~are presented in the uncertainty analysis section.~~

262

4. Results and discussion

264   The average rBC concentration of the campaign was 0.14 μg m^{-3} and the average OA

265 concentration was 1.5 μg m^{-3} (Figure 1). The two major Saharan dust events affected, as expected,

266 the aerosol optical properties. In the present study we focus only on the non-dust periods. The

267 dominant PM$_1$ components were sulfate and OA, accounting for 46% and 34% of the PM$_1$,

268 respectively. The O:C ranged from 0.65 to 1, with an average value of 0.83, revealing the absence

269 of fresh OA. These values are typical in Finokalia during the spring and summer periods

270 (Hidlebrandt et al., 2010).

271

4.1 OA Volatility

273   The estimated volatility distribution for the total OA in Finokalia during FAME-16 is

274 depicted in Figure 2. Use of OA with $C^* = 10^{-8}$ μg m^{-3} was needed to capture the behavior of the

275 OA at 400 °C. Almost 40% of the OA consisted of semi-volatile organic compounds (SVOCs),

276 35% of low volatility organic compounds (LVOCs), and the rest was extremely low volatility

277 organic compounds (ELVOCs).

278   The estimated value of the effective vaporization enthalpy was 80 ± 20 kJ mol^{-1}. This value

279   was in agreement with the reported value by Lee et al. (2010) of 80 kJ mol^{-1} for the FAME-08

280   campaign. The estimated accommodation coefficient was 0.27, ranging from 0.1 to 0.8. This value

281   was a little higher than the 0.05 value reported in the earlier study. However, both suggest only

282   moderate resistances to mass transfer during the evaporation in the TD.

283   The corresponding measured and predicted thermograms are depicted in Figure 3. Almost

284   30% of the OA had not evaporated even after heating at 400 ^{o}C. The temperature at which half of

285   the OA evaporated was T$_{50}$=120 ^{o}C, a value similar to that observed by Lee et al. (2010). The

286   composition of the OA leaving the TD changed significantly as temperature increased according

287   to the model. At 125 ^{o}C the LVOCs and ELVOCs contributed equally to the remaining OA mass.

288   For further temperature increases the LVOC fraction was reduced until 375 ^{o}C, at which point only

289   the ELVOCs remained.

290   PMF analysis resulted in a two-factor solution (Florou et al., in prep.). Factor 1

291   corresponded to more oxidized oxygenated OA (MO-OOA) and Factor 2 to a less oxidized

292   component (LO-OOA). The average contribution of the two factors was 47% for the MO-OOA

293   and 53% for the LO-OOA. The O:C for the MO-OOA was 0.95 (OS$_C$ = 0.59) and for the LO-

294   OOA it was 0.56 (OS$_C$ = -0.27). There was a weak positive correlation between LO-OOA, MO-

295   OOA and rBC. The R^2 between the hourly concentrations of MO-OOA and rBC was 0.12 (Figure

296   S12), and for LO-OOA and rBC 0.17 (Figure S13). This is not unexpected given that Finokalia is

297   far away from the corresponding sources of both BC and organic compounds and significant

298   physical and chemical processing has taken place during the transport of the aerosol from the

299   sources to the receptor.

300   The OA in the Eastern Mediterranean during the summer has significant contributions from

301   both anthropogenic and biogenic sources but their contributions remain uncertain. Based on our

302   recent work (Drosatou et al., 2019) the LO-OOA and MO-OOA do not reflect different sources,

303   but rather different degrees of chemical aging. The Finokalia area is characterized by the absence

304   of local sources and as result the absence of fresh OA. The area is characterized by dry land and

305   dry vegetation (dry bushes), thus no high biogenic emissions are expected. The OA during FAME-

306   08, was also found to consist entirely of OOA with no primary OA (POA) present (Hildebrandt et

307   al., 2010). POA evaporates and gets oxidized rapidly in the photochemically active environment

308   of the Eastern Mediterranean during its transport from its sources to this remote site. FLEXPART

309 simulations during the measurement campaign revealed that the air masses arriving at the site
310 during the study were originating from continental Greece and the Balkans (30% of the time),
311 Aegean (13% of the time), Africa (24%), and Italy/Sicily (33%).

312   The volatility distributions of the two PMF factors were estimated following the same
313 approach as that for the total OA. The measured thermograms for the two PMF factors are shown
314 in Figure 4. Almost 50% of both the MO-OOA and the LO-OOA evaporated at 150 ^{o}C. Almost
315 30% of the MO-OOA mass, and about 20% of the LO-OOA did not evaporate even at temperatures
316 as high as 400°C. The model reproduced the observed MFR values for both factors. Both factors
317 contained components with a wide volatility range. The MO-OOA exhibited a bimodal volatility
318 distribution with peaks at effective saturation concentrations of 10^{-8} and 10 μg m^{-3}. Its effective
319 enthalpy of vaporization was approximately 90 ± 35 kJ mol^{-1} and its accommodation coefficient
320 was 0.27. The estimated volatility distribution of the LO-OOA was a little more uniform peaking
321 at an effective saturation concentration of 1 μg m^{-3}. The average calculated saturation
322 concentration of LO-OOA at 298 K was 0.016 μg m^{-3}, an order of magnitude higher than that of
323 the MO-OOA. The LO-OOA enthalpy of vaporization was 70 ± 20 kJ mol^{-1}, 20 kJ mol^{-1} lower
324 than that of the MO-OOA. Its accommodation coefficient was approximately 0.1 indicating small
325 mass transfer resistances. MO-OOA consisted of approximately 40% SVOCs, 30% LVOCs, and
326 30% ELVOCs. On the contrary, LO-OOA consisted of almost 45% SVOCs, 40% LVOCs and only
327 15% ELVOCs. ELVOCs can be produced both by primary sources (combustion of fossil fuels but
328 also biomass burning) and secondary processes. Given the intense chemical processing of the
329 organic compounds from all sources in their way to Finokalia, we cannot assign based on our
330 measurements to a specific source or process.

331   The fitting of the individual factor thermograms implicitly assumes that each factor had the
332 same size distribution as the total OA and also that the two factors were externally mixed. The
333 uncertainty introduced by these two assumptions was implicitly evaluated comparing the estimated
334 total OA of volatility distribution with the composition-weighted average of the volatility
335 distributions of the two OA factors. The two distributions agreed within a few percent for $10^{-3}<C^{*}<$
336 10^{0} and within 10% for the lowest and highest volatility bins.

337

338

339

4.2 Aerosol optical properties

The PAX was used to measure the b_{abs} and b_{scat} at 405 nm. The measured $b_{scat,405}$ ranged from 11.5 to 47 Mm^{-1} with an average campaign value of 26.5 Mm^{-1} (Figure 5). The corresponding $b_{abs,405}$ ranged from 0.64 to 5.6 Mm^{-1} with an average value of 2.1 Mm^{-1}.

The absorption coefficients measured by the aethalometer at λ=370 nm and at λ=470 nm, were compared with the absorption coefficient measured by the PAX at λ=405 nm. The measurements of the two instruments were highly correlated with R^2=0.9-0.91. The $b_{abs,370}$ measured by the aethalometer was higher than the $b_{abs,405}$ of the PAX. Their relationship is described by the equation y=3.32x - 3.24. Similarly, the $b_{abs,450}$ measured by the aethalometer was higher than that of the PAX at 405 nm and their relationship was described by y=1.85x – 0.93 (Figure S14). Part of these differences are due to the artifacts associated with filter-based absorption measurements (Cappa et al., 2008; Lack et al., 2008).

Acetonitrile is a known biomass burning marker and can help identify the potential influence of the site by biomass burning events or wildfires during the campaign. The acetonitrile concentration measured by the PTR-MS remained close to 0.4 ppb during the campaign, which is the local background level. This together with the low BC levels indicate that the site was not impacted by nearby biomass burning during the study.

The $b_{abs,405}$ variation followed that of the rBC (R^2=0.74 for the hourly averages). The R^2 at λ=370 nm was lower at 0.67 than that at 405 nm. This is consistent with the presence of some BrC. However, the $b_{abs,370}$ is measured by the aethalometer and the $b_{abs,405}$ by the PAX. For the b_{abs} at higher wavelengths measured by the aethalometer the R^2 at λ=450 nm was 0.68, at λ=520 nm 0.67, at λ=590 nm 0.65, at λ=660 nm 0.65, and at λ=950 nm 0.51 ~~-~~(Figure S15). These values are ~~rather~~ inconclusive regarding the existence or absence of BrC. Part of the explanation for this behavior could be that a fraction of the BrC is associated with rBC either from the emissions or from the associated gas-phase pollutants that react in their way to the site.

The ratio of the $b_{abs,405}$, measured by the PAX, over the rBC mass, was equal to ~~dMAC$_{405}$=1~~5~~6.7~~6.7$\pm$2.~~5~~2 m^2 g^{-1}. In this study the average rBC size distribution had a number mode diameter of 67 nm and a mass mode diameter equal to 185 nm. The measured MAC$_{405}$ is clearly higher than the expected MAC$_{405}$ of uncoated BC particles (Bond et al., 2006). The difference between the measured and the reference~~theoretical~~ value of MAC$_{405}$ can be due to the coating of

370 BC by other PM components (lensing effect) and/or the existence of other absorbing material.

371 These two potential explanations will be explored in the following paragraphs.

372 The AAE of the aerosol was calculated using a power-law fitting of the b_{abs} measured by

373 the aethalometer in all seven wavelengths (370, 470, 520, 590, 660, 880, 950 nm). The campaign

374 average AAE was 0.97±0.22. Lack and Cappa (2010) suggested that an AAE>1.6 should confirm

375 the presence of non-BC absorbing material, however an AAE<1.6 does not exclude its presence.

376 The AAE of coated BC cores can deviate from the typical AAE=1 with values greater or lower

377 than unity. Gyawali et al. (2009) ~~using a core-shell model~~ have shown using a core-shell model

378 and assuming spherical particles that for relatively small cores, the coating thickness increase leads

379 to the increase of the AAE while for large cores, AAE is not affected by the changes of the coating

380 thickness. ~~(Gyawali et al., 2009).~~ Liu et al. (2018) showed that the AAE of coated BC is highly

381 sensitive to the particle size distribution and demonstrated that AAE decreases as particle size

382 increases~~-~~. They showed that an AAE as low 0.8 is possible ~~(Liu et al., 2018). The same study~~and

383 demonstrated the importance of various parameters on the BC AAE and the potential problems

384 introduced by assuming BC AAE as being equal to 1.0. Based on the relatively large aged particles

385 present in Finokalia relatively low values of AAE should be expected. According to simulation

386 presented by Gyawali et al. (2009), the average AAE for this study can range from 1 to 1.25, based

387 on the core diameter measured and the estimated coating thickness. Therefore, the relatively low

388 average AAE does not preclude the presence of some absorbing organic aerosol.

389 Mie theory calculations were performed in order to estimate the MAC_{405} and the E_{abs} due

390 to the lensing effect of the shell covering the BC core. In our base case the coating thickness was

391 estimated based on the ratio of the total aerosol mass over ~~the~~ the BC mass (Saliba et al., 2016).

392 Initially, a non-absorbing shell was assumed. The predicted MAC_{405} had an average value of 15.8

393 $m^2\ g^{-1}$. The average E_{abs} due to the lensing effect was 2.13. The predicted average MAC_{405} using

394 the measured BC size distribution and assuming pure uncoated spherical particles was 7.4 $m^2\ g^{-1}$

395 varying from 6.1 to 7.8 $m^2\ g^{-1}$ during the study (hourly averages). This is consistent with the

396 expected 5.3-9.2 $m^2\ g^{-1}$ for BC core diameters in the 10-350 nm size range (Bond et al. 2006). The

397 average predicted MAC_{405} was lower than the average measured MAC_{405} =16 $m^2\ g^{-1}$ but the p-

398 value was equal to 0.079.~~.~~ Taking into account ~~However, based on~~ the measurement uncertainty,

399 the measured average MAC_{405} could range from 14.4 to 17.6 $m^2\ g^{-1}$. However, ~~T~~here were several

400 periods during which the measured MAC was much higher than the predicted values with the

401 differences as high as 8.5 m^2 g^{-1} (Figure 6). These differences~~crepancies~~ suggest the average

402 contribution of BrC to absorption during the measurement period was relatively small, but there

403 were periods with ~~potential presence of~~ high levels of absorbing OA ~~during these periods~~. ~~The~~

404 ~~relationship between the predicted MAC$_{405}$ and the calculated MAC$_{405}$ was investigated using~~

405 ~~statistical t test analysis and found a p= 0.079.~~

406 In the next step, the Mie theory calculations were repeated assuming an absorbing shell

407 with a refractive index of n_{OA} = 1.55 + ki, where the imaginary part, k, was allowed to vary from

408 0 to 0.4. This range of k values was selected based on previous literature (Kirchstetter et al., 2004;

409 Alexander et al., 2008; Chakrabarty et al., 2010; Chen and Bond, 2010; Saleh et al., 2014;

410 Chakrabarty et al., 2016, Li et al., 2016; Saleh et al., 2018). Approximately half of the resulting k

411 values during the campaign were zero, suggesting a non-absorbing shell, while the other half were

412 were positive. More specifically, 24% of the estimated k values ranged from 0.01 to 0.1, 8% from

413 0.11 to 0.2, 3% from 0.21 to 0.3, and 10% of the k values ranged from 0.31 to 0.4. During these

414 periods, the campaign average $b_{abs,405}$ was equal to 2.4 Mm^{-1}. BrC was estimated to lead to a 15%

415 increase of the campaign average $b_{abs,405}$.

416 The Mie calculations were repeated using a coating thickness estimated by the LEO fit

417 method and the SP2 data. The average coating thickness calculated by this approach was

418 approximately half of that calculated using the internal mixture assumption (Figure S11). This

419 resulted in lower predicted absorption and therefore a larger gap between measurements and

420 predictions assuming that the organic aerosol was not absorbing. The predicted MAC$_{405}$ had an

421 average value of 14.4 m^2 g^{-1}. The predicted average MAC$_{405}$ assuming pure uncoated spherical

422 particles was 7.4 m^2 g^{-1}. The E_{abs} was equal to 1.94. Assuming an absorbing ~~shell~~shell, we found

423 that the imaginary part of the refractive index of the shell was 20% of the times in the range of

424 0.01 to 0.1, 16% between 0.11 to 0.2, 16% between 0.21 to 0.3, and 20% between 0.31 to 0.4.

425 Only 28% of the times the k was equal to 0 indicating no absorbing shell.

426 For ~~In~~ both methods used to estimate the MAC$_{405}$ it is noted that there was~~is~~ presence of

427 absorbing material in 45% up to 72% of the measurements.

428

429 **4.3 The role of ELVOCs**

430 ELVOCs can exhibit substantial larger light absorption than LVOCS or SVOCs. The

431 association of photochemically aged BrC with material of lower volatility ~~away from its sources~~

432 has been reported in a number of studies focusing on biomass burning (Saleh et al., 2014; Wong

433 et al., 2019). The hypothesis that the presence of ELVOCs could explain the higher aerosol light

434 absorption was tested. The unexplained MAC (ΔMAC) difference of measured and predicted

435 values was compared with the total ELVOC mass concentration. The ELVOC concentration was

436 estimated based on the results on the volatility analysis of the two PMF factors:

437 $$[ELVOC]= 0.15\ [LO\text{-}OOA] + 0.3\ [MO\text{-}OOA]$$

438 The predicted MAC_{405} used was from the base case Mie~~IE~~ theory calculations in which the coating

439 thickness was estimated from BC mass fraction ~~total aerosol mass over the the BC mass.~~ The

440 unexplained b_{abs} at 405 nm~~,405~~ (3 h average values) was well correlated with the estimated ~~ELVOC~~

441 concentrations with an R^2=0.76 (Figure 7). Even a~~A~~fter excluding the period with the highest

442 unexplained absorption, the relationship is still relatively strong with R^2=0.41. The corresponding

443 R^2 between the 3-h average ΔMAC and the ~~ELVOCs~~ was 0.66 (Figure S16). These results suggest

444 that the ELVOCs were probably contributing to the total absorption and could explain the

445 difference in the MAC.

446 Correlation of the ΔMAC with the rBC, and with other parameters were lower than those

447 for the ELVOCs. For example, the R^2 with the rBC was 0.38, with the LO-OOA 0.44 and with the

448 MO-OOA 0.29. There was a relatively high correlation with the sulfate levels (R^2=0.59) that could

449 be interesting as high sulfate levels in this area correspond to high aerosol acidity which has been

450 shown to promote formation of oligomers in secondary organic aerosol. A comparison of the

451 difference of measured and the predicted $b_{abs,405}$ and the ELVOC was also conducted for all the

452 periods including those in which no BrC was present (k=0). The correlation was $R^2 = 0.52$. During

453 the k=0 periods the predicted $b_{abs,405}$ was equal or higher than the measured $b_{abs,405}$. This difference

454 was due to overestimation of the absorption values by the Mie theory or due to the uncertainties in

455 the measurements of the $b_{abs,405}$.

456 The c~~C~~alculations were repeated using the predicted MAC ~~calculate~~ based on the Mie~~IE~~

457 theory assuming a coating thickness according to the LEO fit. The correlation between the

458 unexplained absorption and the ELVOC concentration remained high with R^2=0.69 (Figure S17),

459 suggesting that despite the uncertainty in the coating thickness our results are quite robust.

460

461 **5. ~~Uncertainty~~ Sensitivity analysis**

The analysis presented in the previous sections has been based on a series of assumptions and, as expected is affected, by measurement uncertainties. We have tested the robustness of our conclusion about the link between the unexplained absorption and ELVOC levels by repeating the analysis for several cases. We focused on the estimation of the coating thickness of the BC particles, the refractive index of black carbon, the uncertainty of the measurements by the SP2 and PAX$_{405}$, the uncertainty of the results from the PMF analysis and finally the uncertainty of the thermodenuder model. The results of the corresponding tests are summarized in the following paragraphs.

~~The coating thickness was recalculated applying the LEO algorithm on the SP2 measurements. The average coating thickness calculated by this approach was approximately half of that calculated using the internal mixture assumption (Fig. S11). This resulted in lower predicted absorption and therefore a larger gap between measurements and predictions assuming that the organic aerosol was not absorbing. The unexplained absorption increased by approximately 35% (from 0.24 to 0.32 Mm^{-1}). The calculations indicated that 71% of the samples had a k>0 suggesting an absorbing shell. The correlation between the unexplained absorption and the ELVOC concentration remained high R^2=0.69 (Fig. S17), suggesting that despite the uncertainty in the coating thickness our results are quite robust.~~

The effect of the assumed BC refractive index on our results was tested by repeating the Mie theory calculations for two additional values: a relatively high value of 1.95~~-+0.6~~79i and a relatively low value 1.5 + 0.5i ~~were assumed~~ (Bond and Bergstrom, 2006). For the high refractive index, the predicted average MAC$_{405}$ using the measured BC size distribution and assuming pure uncoated spherical particles was 7.7 m^2 g^{-1} varying from 6.3 to 8.2 m^2 g^{-1} during the study (hourly averages). Even if the unexplained absorption was reduced its R^2 with the ELVOCs remained high and equal to 0.72 (Fig. S18). For the low refractive index, the predicted average MAC$_{405}$ of the uncoated BC particles was 6.2 m^2 g^{-1} (range of 5.2-6.5 m^2 g^{-1} during the study). The R^2 between the unexplained absorption, $\Delta b_{abs,405}$ and the ELVOC concentration was R^2=0.55 (Fig. S19). The link between the unexplained absorption and the abundance of ELVOCs is quite robust with respect to the assumed value of the BC refractive index.

We estimated that 92-97% of the BC mass concentration was inside the SP2 measurement window therefore given that we also corrected for it fitting the measured size distribution, the uncertainty introduced by this limitation of the SP2 was minor. Nakayama et al. (2015) ~~Lack et al.~~

493 ~~(2012) estimated~~ reported an uncertainty of the ~~*aerosol absorption measurement*~~ b_{abs} ~~,405~~

494 measurements by the PAX of less than 10%. Both of these uncertainties did not have an important

495 effect on the link between the unexplained absorption and the ELVOC concentrations.

496   An assessment of the uncertainty of the concentrations of the two OA factors determined

497 by the PMF analysis was performed by bootstrapping 10 simulations (Ulbrich et al., 2009). The

498 estimated uncertainty for the LO-OOA concentrations was 2% and for the MO-OOA

499 concentrations was 3% (Fig. S20). These relatively small uncertainties suggest that the PMF

500 uncertainty regarding the determination of these factors does not affect significantly the

501 conclusions of this study.

502   The uncertainty related to the volatility distributions determined by the thermodenuder

503 results was assessed by estimating low and high limits of the ELVOC concentrations: $ELVOC_{low}$

504 and $ELVOC_{high}$. These were estimated based on the extreme mass fractions that were calculated

505 during the sensitivity analysis of the TD model (Supplemental information Section S2). The LO-

506 OOA ELVOC mass fraction ranged from 0.09 to 0.25 while that of the MO-OOA from 0.13 to

507 0.47. For the low ELVOC case we thus assumed that:

508        $[ELVOC_{low}] = 0.09\,[LO\text{-}OOA] + 0.13\,[MO\text{-}OOA]$

509 The R^2 between the unexplained $b_{abs,405}$ and $ELVOC_{low}$ was $R^2 = 0.79$ (Fig. S21). For the high

510 ELVOC case:

511        $[ELVOC_{high}] = 0.25\,[LO\text{-}OOA] + 0.47\,[MO\text{-}OOA]$

512 Once more the correlation between the unexplained absorption at 405 nm and the ELVOCs was

513 quite high with $R^2 = 0.78$ (Fig. S22).

514

515 **6. Conclusions**

516   A month-long campaign was conducted at a remote site, in Finokalia, Crete during May of

517 2016. The dominant PM_1 components were sulfate and aged organics with O/C=0.81. The average

518 ambient OA concentration was 1.5 µg m^{-3} and the rBC was 0.14 µg m^{-3}. Continuous monitoring of

519 biomass burning markers revealed that there were no periods of enhanced biomass burning

520 influence on the site during the campaign. PMF analysis resulted in two secondary OA factors:

521 one more oxidized (MO-OOA) and one less oxidized (LO-OOA). Total OA consisted on average

522 of 40% SVOCs, 35% LVOCs and 25% ELVOCs. Both OA components with a wide range of

523 volatilities. Approximately 30% of the MO-OOA was ELVOCs, 30% LVOCs and 40% semi-

524 volatile material. The LO-OOA was more volatile on average with 40% consisting of LVOCs and
525 45% of SVOCs and 15% of ELVOCs.

526   Aerosol optical properties were measured. The average b_{scat} at 405 nm was 26.5 Mm^{-1} and
527 the average b_{abs} at 405 nm was 2.1 Mm^{-1}. Furthermore, the average AAE was 0.97 and the MAC$_{405}$
528 was 15.7. Mie theory calculations were able to reproduce less than half of the measured MAC$_{405}$
529 values assuming core-shell morphology and a non-absorbing shell (k=0). We estimated that the
530 non-absorbing shell was causing an enhancement of the absorption by a factor of 2.1. For the other
531 half of the measurements the presence of an absorbing shell with an average k of 0.18 was needed
532 to explain the measurements.

533   The ELVOCs mass concentration was estimated using the volatility distributions of the
534 two factors. The ELVOC concentration was highly correlated with the unexplained MAC$_{405}$
535 (R^2=0.66) and the unexplained $b_{abs,405}$ (R^2=0.76), defined as the differences of the parameters
536 measured and the ones predicted by Mie theory for k=0. These results suggest that the unexplained
537 absorption in this remote site could be due to a large extent to the extremely low volatility
538 components of the organic aerosol.

539

540 *Data availability.* The data in the study are available from the authors upon request
541 (spyros@chemeng.upatras.gr).

542

543 *Author contributions.* AT conducted the absorption measurements, analysed the results and wrote
544 the paper. EL performed the thermodenuder measurements and analysed the results. KF performed
545 the AMS measurements and analysed the results. AL performed the PTR-MS measurements and
546 analysis. EK was responsible for the OA volatility analysis. CK coordinated the field campaign
547 and assisted with all measurements. NW assisted with all measurements SNP was responsible for
548 the design and coordination of the study and the synthesis of the results. All co-authors contributed
549 to the writing of the manuscript.

550

551 *Competing interests.* The authors declare that they have no conflict of interest.

552

553

554

References

Alexander, D. T. L., Crozier, P. A., and Anderson, J. R.: Brown carbon spheres in East Asian outflow and their optical properties, Science, 321, 833–836, 2008.

An, W. J., Pathak, R. K., Lee, B. H., and Pandis, S. N.: Aerosol volatility measurement using an improved thermodenuder: Application to secondary organic aerosol, J. Aerosol Sci., 38, 305–314, 2007.

Andreae, M. O., and Gelencser, A.: Black carbon or brown carbon? The nature of light-absorbing carbonaceous aerosols, Atmos. Chem. Phys., 6, 3131–3148, 2006.

Arnott, W.P., Moosmüller, H., Sheridan, P. J., Ogren, J. A., Raspet, R., Slaton, W.V., Hand, J. L., Kreidenweis, S. M. and Collett Jr., J. L.: Photoacoustic and filter-based ambient aerosol light absorption measurements: instrument comparison and the role of relative humidity, J. Geophys. Res., 108, 4034–44, 2003

Bond, T. C., and Bergstrom, R. W.: Light absorption by carbonaceous particles: An investigative review, Aerosol Sci. and Technol., 40, 27–67, 2006.

Bond, T. C., Habib, G., and Bergstrom, R. W.: Limitations in the enhancement of visible light absorption due to mixing state, J. Geophys. Res., 111, D20211, 2006.

Bohren, C. F., and Huffman, D. R.: Absorption and scattering of light by small particles. Research supported by the University of Arizona and Institute of Occupational and Environmental Health, New York: Wiley Interscience, 1983.

Bougiatioti, A., Stavroulas, I., Kostenidou, E., Zarmpas, P., Theodosi, C., Kouvarakis, G., Canonaco, F., Prévôt, A. S. H., Nenes, A., Pandis, S. N., and Mihalopoulos, N.: Processing of biomass burning aerosol in the eastern Mediterranean during summertime, Atmos. Chem. Phys., 14, 4793–4807, 2014.

Canagaratna, M. R., Jimenez, J. L., Kroll, J. H., Chen, Q., Kessler, S. H., Massoli, P., Hildebrandt Ruiz, L., Fortner, E.,Williams, L. R., Wilson, K. R., Surratt, J. D., Donahue, N. M., Jayne, J. T., and Worsnop, D. R.: Elemental ratio measurements of organic compounds using aerosol mass spectrometry: characterization, improved calibration, and implications, Atmos. Chem. Phys., 15, 253–272, 2015.

Cappa, C. D., Zhang, X., Russell, L. M., Collier, S., Lee, A. K. Y., Chen, C.-L., Betha, R., Chen, S., Liu, J., Price, D. J., Sanchez, K. J., McMeeking, G. R., Williams, L. R., Onasch, T. B., Worsnop, D. R., Abbatt, J. and Zhang, Q.: Light absorption by ambient black and brown carbon and its dependence on black carbon coating state for two California, USA, cities in winter and summer, J. Geophys. Res.,124, 1550−1577, 2019.

Cappa, C. D., Onasch, T. B., Massoli, P., Worsnop, D. R., Bates, T. S., Cross, E. S., Davidovits, P., Hakala, J., Hayden, K. L., Jobson, B. T., Kolesar, K. R., Lack, D. A., Lerner, B. M., Li, S. M., Mellon, D., Nuaaman, I., Olfert, J. S., Petäjä, T., Quinn, P. K., Song, C., Subramanian, R., Williams, E. J., and Zaveri, R. A.: Radiative absorption enhancements due to the mixing state of atmospheric black carbon, Science, 337, 2012.

Cappa, C., Lack, D., Burkholder, J., and Ravishankara, A.: Bias in filter based aerosol light absorption measurements due to organic aerosol loading: Evidence from laboratory measurements, Aerosol Sci. Technol., 42, 1022–1032, 2008.

Chakrabarty, R. K., Gyawali, M., Yatavelli, R. L. N., Pandey, A., Watts, A. C., Knue, J., Chen, L.-W. A., Pattison, R. R., Tsibart, A., Samburova, V., and Moosmüller, H.: Brown carbon aerosols from burning of boreal peatlands: microphysical properties, emission factors, and implications for direct radiative forcing, Atmos. Chem. Phys., 16, 3033–3040, 2016.

Chakrabarty, R. K., Moosmuller, H., Chen, L.-W. A., Lewis, K., Arnott, W. P., Mazzoleni, C., Dubey, M. K., Wold, C. E., Hao, W. M., and Kreidenweis, S. M.: Brown carbon in tar balls from smoldering biomass combustion, Atmos. Chem. Phys., 10,6363–6370, 2010.Chen, Y. and Bond, T. C.: Light absorption by organic carbon from wood combustion, Atmos. Chem. Phys., 10, 1773–1787, 2010.

China, S., Scarnato, B., Owen, R. C., Zhang, B., Ampadu, M. T. , Kumar, S., Dzepina, K., Dziobak, M. P., Fialho, P., Perlinger, J. A., Hueber, J., Helmig, D., Mazzoleni, L. R., and Claudio Mazzoleni, C.: Morphology and mixing state of aged soot particles at a remote marine free troposphere site: Implications for optical properties, Geophys. Res. Lett., 42, 1243–1250, 2015. Clarke, A. D., Shinozuka, Y., Kapustin, V. N., Howell, S., Huebert, B., Doherty, S., Anderson, T., Covert, D., Anderson, J., Hua, X., Moore, K. G., McNaughton, C., Carmichael, G., and Weber, R.: Size distributions and mixtures of dust and black carbon aerosol in Asian outflow: Physiochemistry and optical properties, J. Geophys. Res., 109, D15S09, doi.org/10.1029/ 2003JD004378, 2004.

Dastanpour, R., Momenimovahed, A., Thomson, K., Olfert, J., and Rogak, S.: Variation of the optical properties of soot as a function of particle mass, Carbon, 124, 201–211, 2017.

Ditas, J., Ma, N., Zhang, Y., Assmann, D., Neumaier, M., Riede, H., Karu, E., Williams, J., Scharffe, D., Wang, Q., Saturno, J., Schwarz, J. P., Katich, J. M., McMeeking, G. R., Zahn, A., Hermann, M., Brenninkmeijer, C. A. M., Andreae, M. O., Pöschl, U., Su, H., and Cheng, Y.: Strong impact of wildfires on the abundance and aging of black carbon in the lowermost stratosphere, P. Natl. Acad. Sci. USA, 115, 11595–11603, 2018.

Donahue, N. M., Robinson, A. L., Stanier, C. O., and Pandis, S. N.: Coupled partitioning, dilution, and chemical aging of semivolatile organics, Environ. Sci. Technol., 40, 2635–2643, 2006.

Drosatou, A. D., Skyllakou, K., Theodoritsi, G. N., and Pandis, S. N.: Positive matrix factorization of organic aerosol: insights from a chemical transport model, Atmos. Chem. Phys., 19, 973–986, https://doi.org/10.5194/acp-19-973-2019, 2019.

Forestieri, S. D., Helgestad, T. M., Lambe, A. T., Renbaum-Wolff, L., Lack, D. A., Massoli, P., Cross, E. S., Dubey, M. K., Mazzoleni, C., Olfert, J. S., Sedlacek Iii, A. J., Freedman, -A., Davidovits, P., Onasch, T. B., and Cappa., C. D.: Measurement and modeling of the

multiwavelength optical properties of uncoated flame-generated soot, Atmos. Chem. Phys., 18 (16), 12141–12159, 2018.

Florou, K., Liangou, A., Louvaris, E., Kaltsonoudis, C., Tasoglou, A., Patoulias, D., Kouvarakis, G., Vlachou, A., Kourtchev, I. and Spyros N. Pandis, S. N.: The Finokalia Aerosol Measurement Experiment (FAME-16): Atmospheric processing of organic aerosol in the Eastern Mediterranean, in prep.

Fuller, K. A., Malm, W. C., and Kreidenweis, S. M.: Effects of mixing on extinction by carbonaceous particles, J. Geophys. Res., 104, 15941–15954, 1999.

Gao, R. S., Schwarz, J. P., Kelly, K. K., Fahey, D. W., Watts, L. A., Thompson, T. L., Spackman, J. R., Slowik, J. G., Cross, E. S., Han, J. H., Davidovits, P., Onasch, T. B., and Worsnop, D. R.: A novel method for estimating light-scattering properties of soot aerosols using a modified single-particle soot photometer, Aerosol Sci. Technol., 41, 125–135, 2007.

Gkatzelis, G. I., Papanastasiou, D. K., Florou, K., Kaltsonoudis, C., Louvaris, E. and Pandis, S. N.: Measurement of nonvolatile particle number size distribution, Atmos. Meas. Tech., 9, 103–114, 2016.

Gyawali, M., Arnott, W. P., Lewis, K., and Moosmueller, H.: In situ aerosol optics in Reno, NV, USA during and after the summer 2008 California wildfires and the influence of absorbing and non-absorbing organic coatings on spectral light absorption, Atmos. Chem. Phys., 9, 8007–8017, 2009.

Gysel, M., Laborde, M., Olfert, J. S., Subramanian, R., and Gröhn, A. J.: Effective density of Aquadag and fullerene soot black carbon reference materials used for SP2 calibration, Atmos. Meas. Tech., 4, 2851–2858, 2011.

Healy, R. M., Wang, J. M., Jeong, C.-H., Lee, A. K. Y., Willis, M. D., Jaroudi, E., Zimmerman, N., Hilker, N., Murphy, M., Eckhardt, S., Stohl, A., Abbatt, J. P. D., Wenger, J. C., and Evans, G. J.: Light-absorbing properties of ambient black carbon and brown carbon from fossil fuel and biomass burning sources, J. Geophys. Res., 120, 6619–6633, 2015.

Hildebrandt, L., Engelhart, G. J., Mohr, C., Kostenidou, E., Lanz, V. A., Bougiatioti, A., DeCarlo, P. F., Prévôt, A. S. H., Baltensperger, U., Mihalopoulos, N., Donahue, N. M., and Pandis, S. N.: Aged organic aerosol in the eastern Mediterranean: The Finokalia aerosol measurement experiment 2008, Atmos. Chem. Phys., 10, 4167–4186, 2010.

Hildebrandt, L., Kostenidou, E., Lanz, V. A., Prévôt, A. S. H., Baltensperger, U., Mihalopoulos, N., Laaksonen, A., Donahue, N. M., and Pandis, S. N.: Sources and atmospheric processing of organic aerosol in the Mediterranean: Insights from aerosol mass spectrometer factor analysis, Atmos. Chem. Phys., 11, 12499–12515, 2011.

Jacobson, M. Z.: Strong radiative heating due to the mixing state of black carbon in atmospheric aerosols, Nature, 409, 695–697, 2001.

Kalivitis, N., Bougiatioti, A., Kouvarakis, G., and Mihalopoulos, N.: Long term measurements of atmospheric aerosol optical properties in the Eastern Mediterranean, Atmos. Res., 102, 351–357, 2011.

Karnezi, E., Riipinen, I., and Pandis, S. N.: Measuring the atmospheric organic aerosol volatility distribution: a theoretical analysis, Atmos. Meas. Tech., 7, 2953–2965, doi:10.5194/amt7-2953-2014, 2014.

Kirchstetter, T., Novakov, T., and Hobbs, P.: Evidence that the spectral dependence of light absorption by aerosols is affected by organic carbon, J. Geophys. Res., 109, D21208, doi.org/10.1029/2004JD004999, 2004.

Kirchstetter, T. W., and Novakov, T.: Controlled generation of black carbon particles from a diffusion flame and applications in evaluating black carbon measurement methods, Atmos. Environ., 41, 1874–1888, 2007.

Knox, A., Evans, G. J., Brook, J. R., Yao, X., Jeong, C.-H., Godri, K. J., Sabaliauskas, K., and Slowik, J. G.: Mass absorption cross-section of ambient black carbon aerosol in relation to chemical age, Aerosol Sci. Tech., 43, 522-532, 2009.

Kostenidou, E., Pathak, R. K., and Pandis, S. N.: An algorithm for the calculation of secondary organic aerosol density combining AMS and SMPS data, Aerosol Sci. Tech., 41, 1002–1010, 2007.

Kouvarakis, G., Tsigaridis, K., Kanakidou, M., and Mihalopoulos, N.: Temporal variations of surface regional background ozone over Crete Island in the Southeast Mediterranean, J. Geophys. Res., 105, 399–407, 2000.

Lack, D. A., Langridge, J. M., Bahreini, R., Cappa, C. D., Middlebrook, A. N., and Schwarz, J. P.: Brown carbon and internal mixing in biomass burning particles, Proc. Natl. Acad. Sci. USA, 109, 14802–14807, 2012.

Lack, D. A., and Cappa, C. D.: Impact of brown and clear carbon on light absorption enhancement, single scatter albedo and absorption wavelength dependence of black carbon, Atmos. Chem. Phys., 10, 4207–4220, 2010.

Lack, D. A., Cappa, C. D., Covert, D. S., Baynard, T., Massoli, P., Sierau, B., Bates, T. S., Quinn, P. K., Lovejoy, E. R., and Ravishankara, A. R.: Bias in filter based aerosol light absorption measurements due to organic aerosol loading: Evidence from ambient measurements, Aerosol Sci. Technol., 42, 1033–1041, 2008.Lanz, V. A., Alfarra, M. R., Baltensperger, U., Buchmann, B., Hueglin, C., and Prévôt, A. S. H.: Source apportionment of submicron organic aerosols at an urban site by factor analytical modelling of aerosol mass spectra, Atmos. Chem. Phys., 7, 1503–1522, 2007.

Lee, B. H., Kostenidou, E., Hildebrandt, L., Riipinen, I., Engelhart, G. J., Mohr, C., Decarlo, P. F., Mihalopoulos, N., Prévôt, A. S. H., Baltensperger, U., and Pandis, S. N.: Measurement of the ambient organic aerosol volatility distribution: Application during the Finokalia Aerosol Measurement Experiment (FAME-2008), Atmos. Chem. Phys., 10, 12149–12160, 2010.

Lelieveld, J., Berresheim, H., Borrmann, S., Crutzen, P. J., Dentener, F. J., Fischer, H., Feichter, J., Flatau, P. J., Heland, J., Holzinger, R., Korrmann, R., Lawrence, M. G., Levin, Z., Markowicz, K. M., Mihalopoulos, N., Minikin, A., Ramanathan, V., de Reus, M., Roelofs, G. J., Scheeren, H. A., Sciare, J., Schlager, H., Schultz, M., Siegmund, P., Steil, B., Stephanou, E. G., Stier, P., Traub, M., Warneke, C., Williams, J., and Ziereis, H.: Global air pollution crossroads over the mediterranean, Science, 298, 794–799, 2002.

Li, X., Chen, Y., and Bond, T. C.: Light absorption of organic aerosol from pyrolysis of corn stalk, Atmos. Environ. 144, 249–256, 2016.

Liu, S., Aiken, A. C., Gorkowski, K., Dubey, M. K., Cappa, C. D., Williams, L. R., Herndon, S. C., Massoli, P., Fortner, E. C., Chhabra, P. S., Brooks, W. A., Onasch, T. B., Jayne J. T., Worsnop, D. R., China, S., Sharma, N., Mazzoleni, C., Xu, L., Ng, N. L., Liu, D., Allan, J. D., Lee, J. D., Fleming, Z. L., Mohr, C., Zotter, P., Szidat, S., and Prévôt, A. S. H.: Enhanced light absorption by mixed source black and brown carbon particles in UK winter, Nat Commun., 6, 843, 2015.

Liu, C., Chung, C. E., Yin, Y., Schnaiter, M.: The absorption Ångström exponent of black carbon: from numerical aspects, Atmos. Chem. Phys., 18, 16409–16418, 2018.

Liu, D., Whitehead, J., Alfarra, M. R., Reyes-Villegas, E., Spracklen, D. V., Reddington, C. L., Kong, S., Williams, P. I., Ting, Y.-C., Haslett, S., Taylor, J. W., Flynn, M. J., Morgan, W. T., McFiggans, G., Coe, H., and Allan, J. D.: Black-carbon absorption enhancement in the atmosphere determined by particle mixing state, Nat. Geosci., 10, 184–188, 2017.

Louvaris, E. E., Florou, K., Karnezi, E., Papanastasiou, D. K., Gkatzelis, G. I., and Pandis, S. N.: Volatility of source apportioned wintertime organic aerosol in the city of Athens, Atmos. Environ., 158, 138-147, 2017.

McMeeking, G. R., Fortner, E., Onasch, T. B., Taylor, J. W., Flynn, M., Coe, H., and Kreidenweis, S. M.: Impacts of nonrefractory material on light absorption by aerosols emitted from biomass burning, J. Geophys. Res., 119, 12272–12286, 2014.

Mihalopoulos, N., Stephanou, E., Kanakidou, M., Pilitsidis, S., and Bousquet, P.: Tropospheric aerosol ionic composition in the eastern Mediterranean region, Tellus, 49B, 314–326, 1997.

Mullins, J., and Williams, A.: The optical properties of soot: A comparison between experimental and theoretical values, Fuel, 66, 277–280, 1987.

Nakayama, T., Suzuki, H., Kagamitani, S., Ikeda, Y., Uchiyama, A., and Matsumi, Y.: Characterization of a three Wavelength Photoacoustic Soot Spectrometer (PASS-3) and a Photoacoustic Extinctiometer (PAX). J. Meteorol. Soc. Japan., 93, 285–308, 2015.

Paatero, P., and Tapper, U.: Positive matrix factorization: A non-negative factor model with optimal utilization of error estimates of data values, Environmetrics, 5, 111–126, 1994.

Park, K., Kittelson, D. B., Zachariah, M. R., and McMurry, P. H.: Measurement of inherent material density of nanoparticle agglomerates, J. Nanopart. Res., 6, 267–272, 2004.

Pikridas, M., Bougiatioti, A., Hildebrandt, L., Engelhart, G. J., Kostenidou, E., Mohr, C., Prevót, A. S. H., Kouvarakis, G., Zarmpas, P., Burkhart, J. F., Lee, B.-H., Psichoudaki, M., Mihalopoulos, N., Pilinis, C., Stohl, A., Baltensperger, U., Kulmala, M., and Pandis, S. N.: The Finokalia Aerosol Measurement Experiment – 2008 (FAME-08): an overview, Atmos. Chem. Phys., 10, 6793–6806, 2010.

Radney, J. G., You, R., Ma, X., Conny, J. M., Zachariah, M. R., Hodges, J. T., and Zangmeister, C. D.: Dependence of Soot Optical Properties on Particle Morphology: Measurements and Model Comparisons, Environ. Sci. Technol., 48, 3169–3176, 2014.

Riipinen, I., Pierce, J. R., Donahue, N. M., and Pandis, S. N.: Equilibration time scales of organic aerosol inside thermodenuders: Kinetics versus equilibrium thermodynamics, Atmos. Environ., 44, 597–607, 2010.

Saleh, R., Cheng, Z., and Atwi., K.: The brown–black continuum of light-absorbing combustion aerosols, Environ. Sci. Technol. Lett. 5, 508–13, 2018.

Saleh, R., Robinson, E. S., Tkacik, D. S., Ahern, A. T., Liu, S., Aiken, A. C., Sullivan, R. C., Presto, A. A., Dubey, M. K., Yokelson, R. J., Donahue, N. M., and Robinson, A. L.: Brownness of organics in aerosols from biomass burning linked to their black carbon content, Nat. Geosci., 7, 647–650, 2014.

Saliba, G., Subramanian, R., Saleh, R., Ahern, A. T., Lipsky, E. M., Tasoglou, A., Sullivan, R. C., Bhandari, J., Mazzoleni, C., and Robinson, A. L.: Optical properties of black carbon in cookstove emissions coated with secondary organic aerosols: Measurements and modeling, Aerosol Sci. Technol., 50, 1264–1276, 2016.

Tasoglou, A., Saliba, G., Subramanian, R., and S. N. Pandis S. N.: Absorption of chemically aged biomass burning carbonaceous aerosol, J. Aerosol. Sci., 113, 141–52, 2017.

Ulbrich, I. M., Canagaratna, M. R., Zhang, Q., Worsnop, D. R., and Jimenez, J. L.: Interpretation of organic components from Positive Matrix Factorization of aerosol mass spectrometric data, Atmos. Chem. Phys., 9, 2891–2918, 2009.

Vrekoussis, M., Liakakou, E., Koçak, M., Kubilay, N., Oikonomou, K., Sciare, J., and Mihalopoulos, N.: Seasonal variability of optical properties of aerosols in the eastern Mediterranean, Atmos. Environ., 39, 7083-7094, 2005.

Weingartner, E., H. Saathoff, M. Schnaiter, N. Streit, B. Bitnar, and U. Baltensperger: Absorption of light by soot particles: Determination of the absorption coefficient by means of aethalometers, J. Aerosol. Sci. 34, 1445–63, 2003.

Wong, J. P. S., Tsagkaraki, M., Tsiodra, I., Mihalopoulos, N., Violaki, K., Kanakidou, M., Sciare, J., Nenes, A., and Weber, R. J.: Atmospheric evolution of molecular-weight-separated brown carbon from biomass burning, Atmos. Chem. Phys., 19, 7319–7334, https://doi.org/10.5194/acp-19-7319-2019, 2019.Wu, J.-S., Krishnan, S. S., and Feath, G. M.: Refractive indices at visible wavelengths of soot emitted from buoyant turbulent diffusion flames, J. Heat Transfer, 119, 230–237, 1997.

Zanatta, M., Laj, P., Gysel, M., Baltensperger, U., Vratolis, S., Eleftheriadis, K., Kondo, Y., Dubuisson, P., Winiarek, V., Kazadzis, S., Tunved, P., and Jacobi, H. W.: Effects of mixing state on optical and radiative properties of black carbon in the European Arctic, Atmos. Chem. Phys., 18, 14037-14057, 2018.

Zhang, Y.; Favez, O.; Canonaco, F.; Liu, D.; Močnik, G.; Amodeo, T.; Sciare, J.; Prévôt, A. S. H.; Gros, V., and Albinet, A.: Evidence of major secondary organic aerosol contribution to lensing effect black carbon absorption enhancement, NPJ Climate and Atmospheric Science, 1, doi.org/10.1038/s41612-018-0056-2, 2018a.

Zhang, Y., Zhang, Q., Cheng, Y., Su, H., Li, H., Li, M., Zhang, X., Ding, A., and He, K.: Amplification of light absorption of black carbon associated with air pollution, Atmos. Chem. Phys., 18, 9879–9896, 2018b.
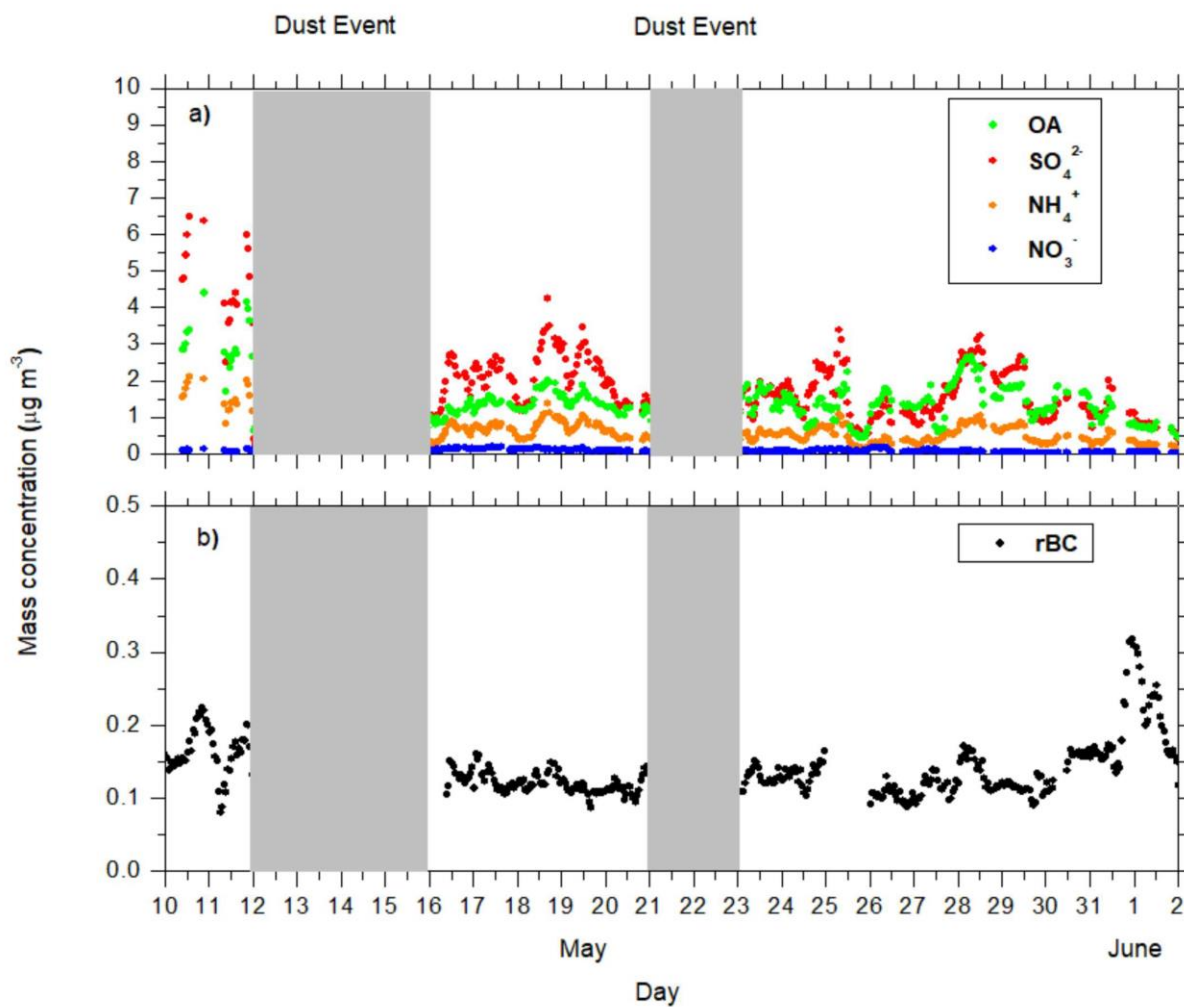
Figure 1: Evolution of the aerosol chemical composition based on the HR-TOF-AMS and SP2 measurements during FAME-16: a) the non-refractory aerosol components; b) rBC concentration. The shaded areas represent the dust events periods.
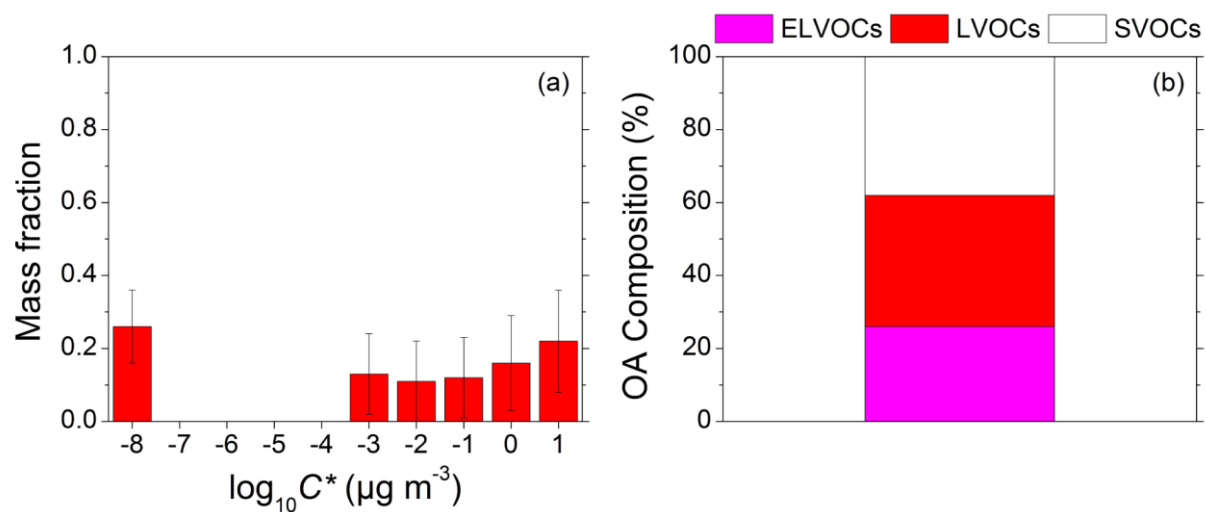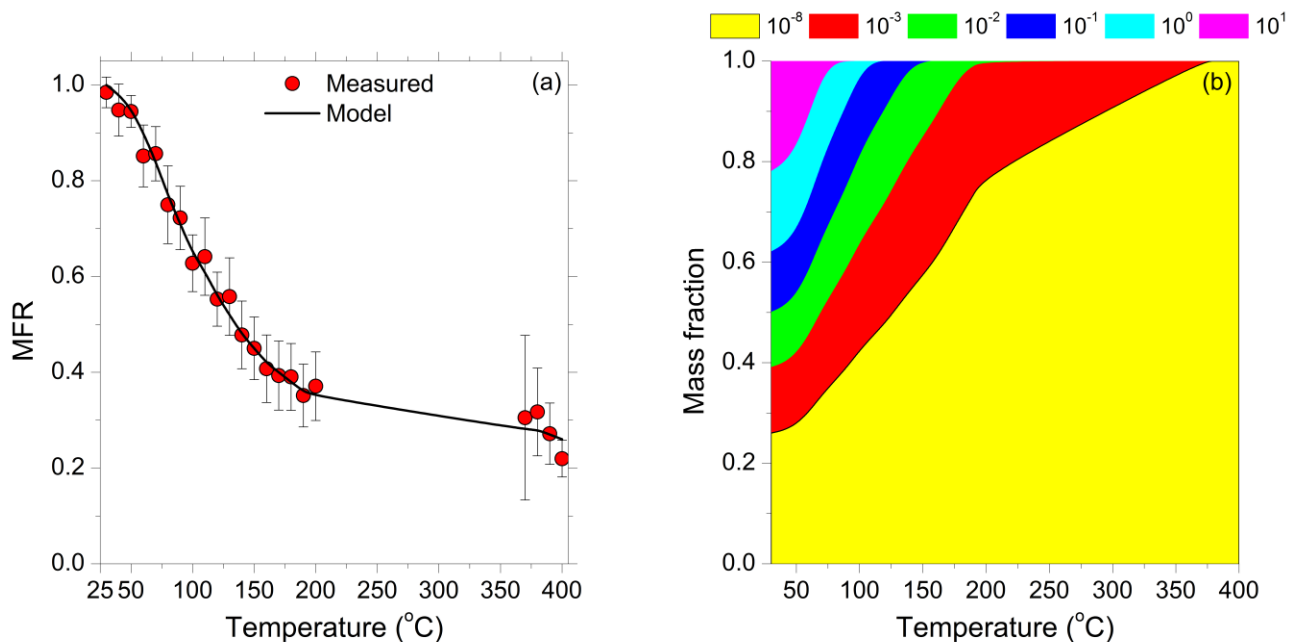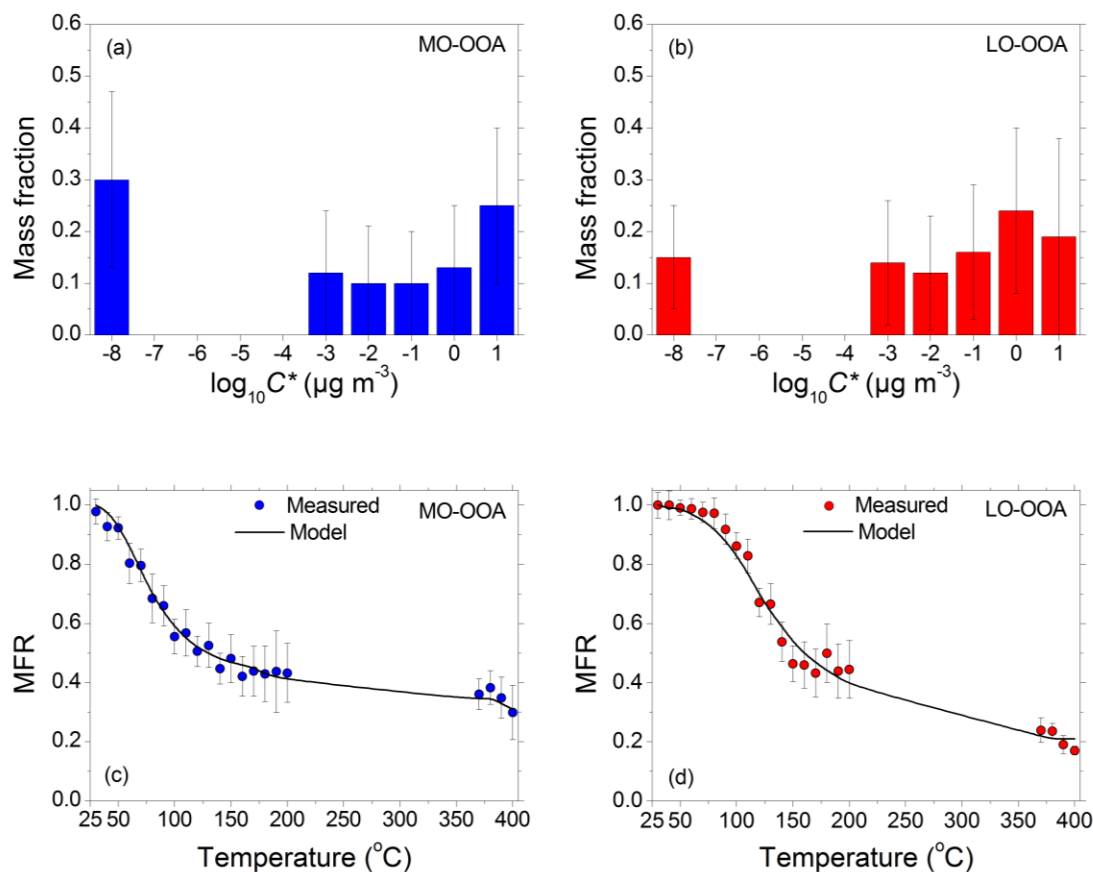
805

Figure 2: (a) Total OA volatility distribution along with its uncertainty estimated by the Karnezi et al. (2014) approach. The error bars represent the corresponding variability (± 1 standard deviation). (b) OA composition. Magenta color represents the ELVOCs, red the LVOCs, and white the SVOCs.

810

Figure 3: (a) Average loss-corrected total OA thermograms. Red circles represent the measured total OA MFR and the error bars the corresponding variability (±2 standard deviations of the mean). The solid lines are the model predictions (b) Mass fraction of the total OA for different effective saturation surrogate species with concentrations as a function of TD temperature. Yellow color represents the contribution of the effective saturation concentration $C* = 10^{-8}$ µg m^{-3}, red the contribution of the $C* = 10^{-3}$ µg m^{-3}, green the $C* = 10^{-2}$ µg m^{-3}, blue the $C* = 10^{-1}$ µg m^{-3}, cyan the $C* = 10^0$ µg m^{-3}, and magenta the $C* = 10$ µg m^{-3}.

818

Figure 4: (a) Estimated volatility distribution of the MO-OOA factor along with its corresponding uncertainties by using the approach of Karnezi et al. (2014). (b) Estimated volatility distribution of the LO-OOA factor along with its corresponding uncertainties. (c) Measured (in circles) and predicted thermograms for the LO-OOA factor. The error bars represent ± 2 standard deviations of the mean. (d) Measured (in circles) and predicted thermograms for the LO-OOA factor. The error bars represent ± 2 standard deviations of the mean.
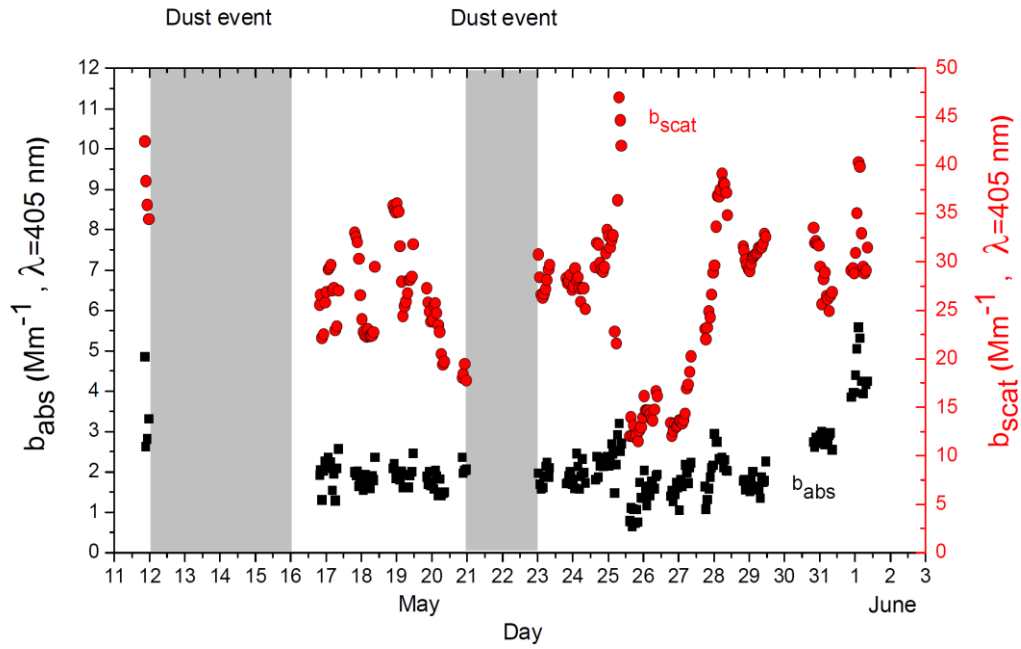
Figure 5: The timeseries of the aerosol optical properties at λ=405 nm. The black squares represent the absorption coefficient, b_{abs}, while the red circles represent the scattering coefficient, b_{scat}. The shaded areas represent the dust events periods.
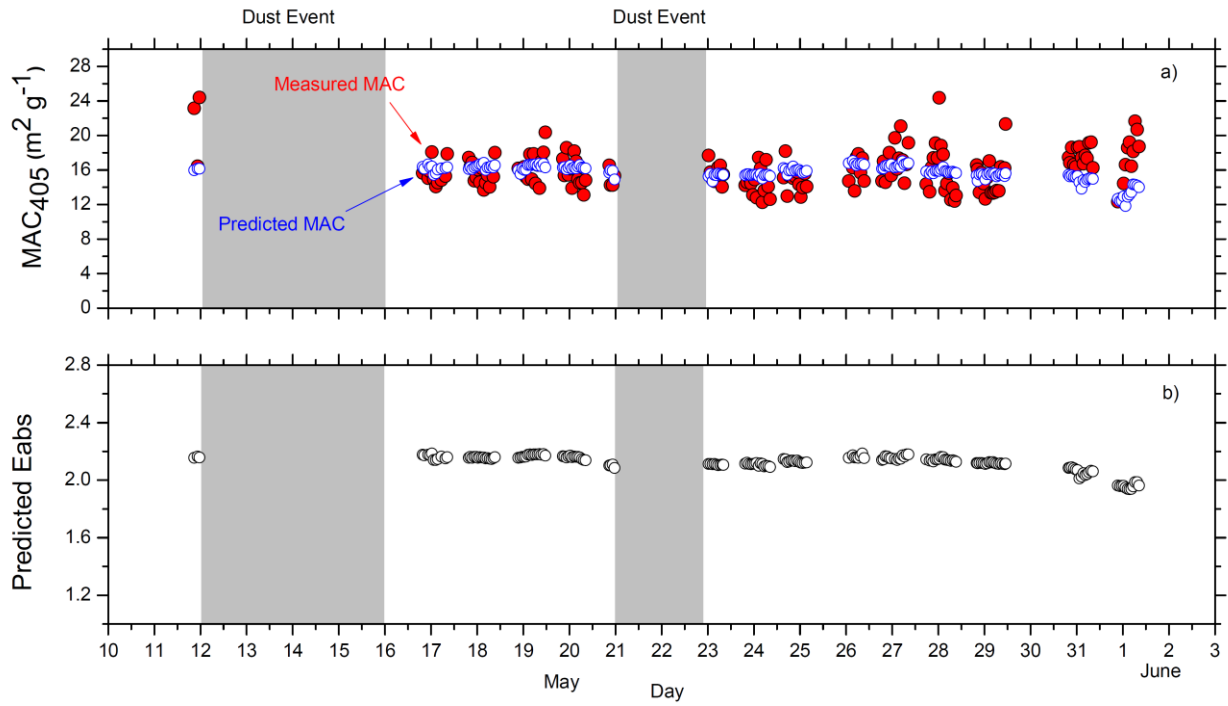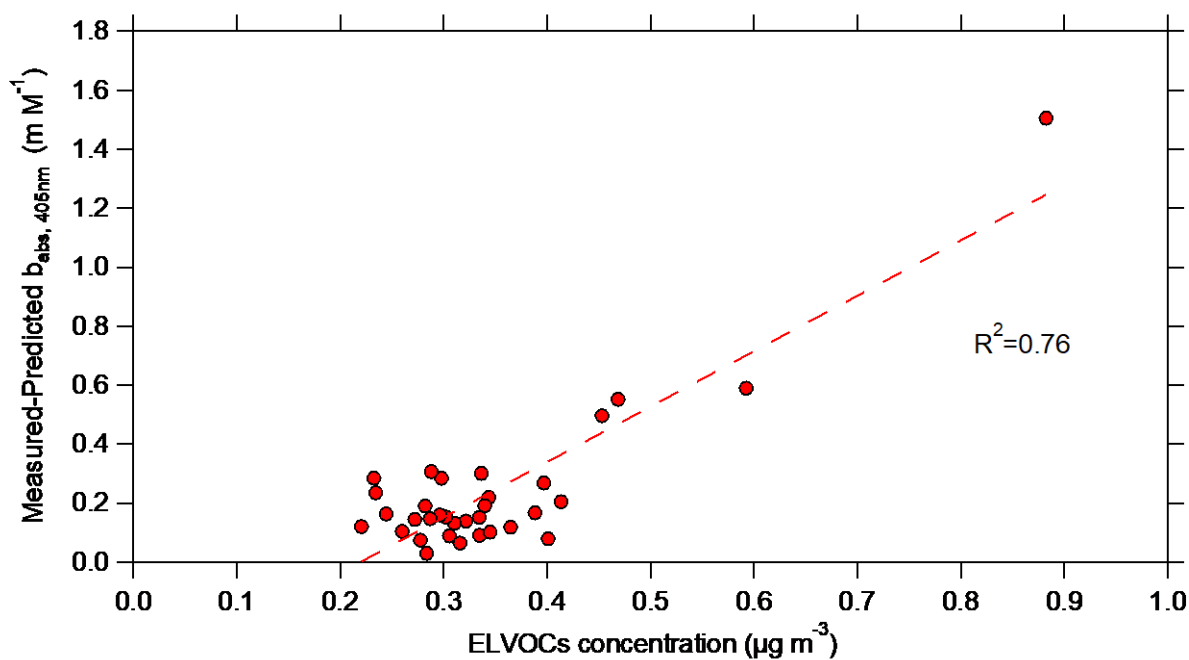
Figure 6: Hourly averaged results from the Mie theory calculations, assuming a non-absorbing shell (k=0): a) predicted (blue circles) and measured MAC_{405} (red circles). b) Hourly averaged Predicted E_{abs} values. The shaded areas represent the dust events periods.

834

835

836 **Figure 7:** a) The difference between the measured and the predicted unexplained $b_{abs,405}$ as a function of
837 the estimated concentration of the ELVOCs. The data shown represent 3-hours averaged values.